3D convection in a fractured porous medium : influence of fracture network parameters

V. Mourzenko[a], C. Mezon[b,c], J.-F. Thovert[a], R. Antoine[e], F. J. Fontaine[d], A. Finizola[c], P.M. Adler[b]

[a] *Institut Pprime, CNRS, SP2MI, Futuroscope Chasseneuil*
[b] *UPMC - Metis, Paris*
[c] *Université de La Réunion - LGSR - IPGP, Saint-Denis la Réunion*
[d] *IPGP, La Plaine des Cafres, la Réunion*
[e] *CEREMA, Rouen*

Keywords: fractured porous medium, heat transfer, convection

1. Introduction

In the crust, fractures/faults can provide preferential pathways for fluid flow or act as barriers preventing the flow across these structures. In hydrothermal systems (usually found in fractured rock masses), these discontinuities may play a critical role at various scales, controlling fluid flows and heat transfer. The thermal convection is numerically computed in 3D fluid satured isotropically fractured porous media. Fractures are 2D convex polygons randomly located in a porous matrix. The fluid is assumed to satisfy 2D and 3D Darcy's law in the fractures and in the porous medium, respectively.

Flow equations are written in a quasi-steady approximation without phase changes and the density of the fluid is supposed to be constant except in the body force term (the Boussinesq approximation). A mass conservation equation and Darcy law describe the flow in porous matrix and in fractures

$$\nabla \cdot \bar{\mathbf{v}} = 0, \quad \bar{\mathbf{v}} = -\frac{1}{\mu} K \left(\nabla P - \rho_F \mathbf{g} \right), \quad \nabla_S \cdot \mathbf{q} + [\bar{\mathbf{v}}] \cdot \mathbf{n} = 0, \quad \mathbf{q} = -\frac{1}{\mu} \sigma_f \left(\nabla_S P - \rho_F \mathbf{g} \right) \tag{1}$$

where P is pressure, $\bar{\mathbf{v}}$ seepage velocity, ρ_F fluid denisity, $\mu = 10^3$ Pa.s viscosity, $\mathbf{g} = 9.81$ m/s^2 gravity acceleration, $K = 10^{-11}$ m^2 bulk permeability, $\sigma_f = b^3/12 = 8.33 \cdot 10^{-11}$ m^3 fracture transmissivity, $b = 10^{-3}$ m fracture aperture. ∇_S two–dimensional gradient operator in a fracture plane, $\mathbf{q}$ flow rate per unit width, $\mathbf{n}$ unit normal vector to the fracture and $[f]$ jump in f between two sides of the fracture.

The energy balance equations in matrix and in fractures read

$$\frac{\partial}{\partial t} \left(\varepsilon \rho_F h_F^* + (1-\varepsilon) \rho_s h_s^* \right) + \nabla \cdot (\bar{\mathbf{v}} \rho_F h_F^*) - \nabla \cdot (\lambda_m \nabla T) = 0, \quad h_s^* = c_s T, \quad h_F^* = c_F T \tag{2}$$

$$\frac{\partial \left(b \rho_F h_{Ff}^* \right)}{\partial t} + \nabla_S \cdot \left(\mathbf{q} \rho_F h_{Ff}^* \right) - \nabla_S \cdot (\Lambda \nabla_S T_f) + [\bar{\mathbf{v}} \rho_F h_F^* - \lambda_m \nabla T] \cdot \mathbf{n} = 0, \quad h_{Ff}^* = c_F T_f \tag{3}$$

where $c_F = 4.2 \cdot 10^3$ and $c_s = 0.9 \cdot 10^3$ J/kg K are specific heat capacities (fluid and solid phase), $\lambda_m = 2.9$ W/m K effective conductivity of porous medium, T and T_f are temperatures of saturated porous medium and of fluid in fractures, respectively, $\varepsilon = 0.1$ porosity, $\rho_s = 3 \cdot 10^3$ kg/m^3 solid matrix density, $\Lambda = b\lambda_F = 0.6 \cdot 10^{-3}$ W/K fracture thermal transmissivity, λ_F =0.6 W/m K fluid thermal conductivity. Fluid density varies with temperature $\rho_F = \rho_0 \left[1 - \alpha_F \left(T - T_0 \right) \right]$. with thermal coefficient of volume expanson $\alpha_F = 2.07 \cdot 10^4$ K^{-1}, $\rho_0 = 10^3$ kg/m^3.

A bounded cubic three-dimensional volume L^3 of porous fractured medium is heated from below. The vertical boundaries are adiabatic and impermeable. The bottom of the box is impermeable while the top could be impermeable or permeable. In open-top cases, a constant pressure P_0 is imposed, while in closed-top cases a no-flow boundary condition is used. A constant temperature T_0 is imposed at the

top of the box; temperature at the bottom is fixed at $T_0 + \Delta T$. In most cases the simulations start from a homogeneous temperature field and immobile fluid. The Rayleigh and Nusselt numbers

$$\mathrm{Ra} = \frac{\alpha_F \rho_0^2 c_F g \Delta T K L}{\mu \lambda_m}, \quad \mathrm{Nu} = \frac{Q_T}{\lambda_m L \Delta T} \tag{4}$$

characterize the system; here Q_T is thermal flux in z-direction through the unit cell.

Simulations have been performed with fracture networks made of squares circumscribed by disks of radius $R = L/5$. Network densities are characterized by $\rho' = N_f V_{ex}/L^3$ [1]. Fractures are inserted in the porous matrix according to the procedure detailed by [1]. The finite volume method and unstructured grids with discretization $\delta_m = R/6$ are used in order to solve the flow and energy transport equations [2]. A variant of flux–corrected method and a time implicit, first order discretization are applied. The Rayleigh number in the porous matrix is the same in every simulation, Ra_m=41.5.

2. Results

Vertical cross sections in Fig. 1a-c demonstrate the temperature field for various fracture transmissivities. For $\sigma' = 0.1$ (Fig. 1a) the presence of fractures does not perturb the system. When σ' increases, a 3D convective behavior develops. The strength of the convection increases with σ', as it can be seen in Fig. 1d that shows the Nu as a function of σ'.

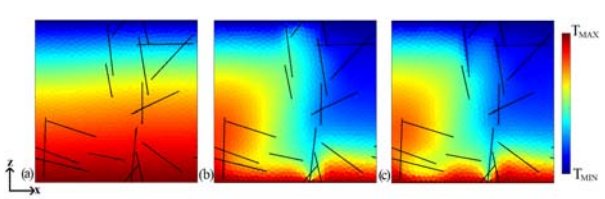

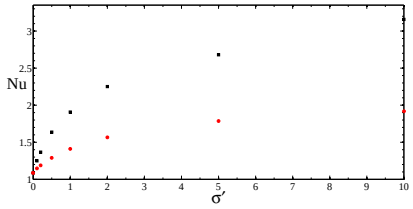

(d)

Figure 1: Temperature fields at steady state for $\sigma' = 0.1$ (a), 5 (b) and 10 (c), and Nu as a function of σ' (d) for Ra_m = 41.5. Data are for $\rho' = 4$ in (a-c) and for $\rho' = 1$ (red symbols) and 4 (black symbols), in (d).

The intensity of convection increases also with ρ' (Fig. 2). One can observe in Fig. 2a-c a thinning of the upflowing plume when ρ' incrases. Nusselt number Nu grows with ρ' almost linearly (Fig. 2d).

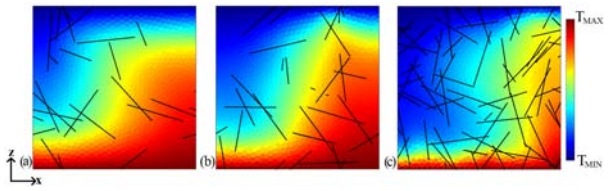

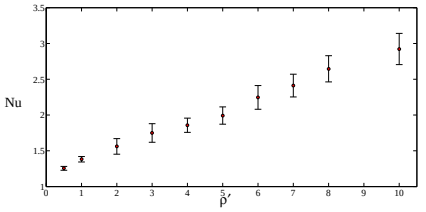

(d)

Figure 2: Temperature fielsd at steady state for $\rho' = 4$ (a), 6 (b) and 10 (c), and Nu as a function of ρ' (d) for Ra_m = 41.5 and $\sigma' = 1$. Data points in (d) are averages over 15 relizations, error bars correspond to standard deviations.

The results of simulations in fractured porous media have been compared with those performed for the porous media with effective transport characteristics. Effective permeability K_{eff} is evaluated and then substituted as permeability of the medium without fractures. The corresponding effective thermal conductivity is found not to differ significantly from the matrix one and the latter value is used.

It has been observed that when Nu_{por} in corresponding effective porous medium is low (≤ 2), the effective approach gives good results, that is Nu_{fr} in fractured porous medium does not differ significantly from Nu_{por}. However, when Nu_{por} increases, for more and more realizations Nu_{fr} deviates from Nu_{por} by about 25%. The difference between the results of simulations in fractured media and those in effective ones is maximal for densities $2 < \rho' < 5$, *i.e.* roughly near the percolation threshold ρ'= 2.3. The effective approach is in agreement with the discretely fractured approach for very low and very high densities of fractures.

References

[1] Huseby O., J.-F. Thovert & P.M. Adler, Geometry and topology of fracture systems, *J. Phys. A*, 30, 1415-1444 (1997).

[2] Bogdanov I., V. Mourzenko, J.-F. Thovert & P.M. Adler, Effective permeability of fractured porous media in steay-state flow, *Water Resourc. Res.*, 39, 1023, doi:10.1029/2001WR000756 (2003).